ADVANCED FUNCTIONAL MATERIALS
www.afm-journal.de

Self-Healing and Antifouling Multifunctional Coatings Based on pH and Sulfide Ion Sensitive Nanocontainers

Zhaoliang Zheng, Xing Huang, Matthias Schenderlein, Dimitriya Borisova, Rong Cao, Helmuth Möhwald, and Dmitry Shchukin*

Application of mesoporous silica nanoparticles (MSNs) as delivery tools for self-healing coatings is limited by spontaneous leakage and specifically responsive release of small molecular inhibitors. In this work, a pH/sulfide ion responsive release system based on MSNs using a Cu-BTA complex forms at the openings of the mesopores into which BTA (corrosion inhibitor) and benzalkonium chloride (biocide) are loaded. The spontaneous leakage of active species is completely avoided and premature release of the loaded composition was lowered to 0.02. The responsive release begins when the pH is lower than 5 or [S^{2-}] is higher than 0.02 mM (about 0.6 ppm). The hybrid coating containing the responsive release system exhibits feedback self-healing property sensitive to lowering of pH and sulfide ion concentration and, at the same time, provides a high barrier level for a long time. Due to incorporation of biocide in the release system, the coating is also provided with antifouling properties.

1. Introduction

In the last decade, considerable progress has been made in controlled delivery of active molecules, especially in molecularly targeted therapy[1] and feedback anti-corrosion coatings[2] by utilizing nanocapsules like mesoporous silica nanoparticles (MSNs) which have large area-to-volume ratio, tunable pore size and regular porous structure.[3] Compared with molecularly targeted therapy in which the stimuli-responsive design of functionalized MSNs has covered almost all kinds of commands, such as temperature changes,[4] pH changes,[5] redox activation,[6] light initiation,[7] and other external stimuli,[8] the application of MSNs in feedback coatings is at a very early stage. The application of MSNs as delivery tools in self-healing coatings is limited by spontaneous leakage of small molecular inhibitors from MSNs during the procedure of forming nanovalves and premature release when loaded MSNs were transferred into the coating matrix.[2b] Biomedicine is also facing the same problem[9] and very few successful examples can be found for encapsulation of small molecular weight drugs with size lower than 1 nm.[10] The other difficulty is to realize stimulated release of inhibitors responsive to certain triggers, especially to pH changes and corrosive (e.g., sulfide)[11] ions. It is also impossible to "borrow tools" from biomedicine (supramolecular nanovalves, sensitive linkers and expensive NPs)[12] to mechanize MSNs for the need of stimuli-triggered release for self-healing anti-corrosion coatings. The supramolecular nanovalves and sensitive linkers are obviously unsuited because of involvement of tedious and intricate steps, vulnerability of sensitive linkers and unpredictable diverse influence of shedding organic compounds in the coating matrix.[13] It is also unacceptable to bind gold NPs[14] and CdS quantum dots[15] to block the release of corrosion inhibitors due to the high cost of the resulting coatings. Therefore, it is of top priority to find a novel, facile and green method to minimize the spontaneous leakage and form a stimuli-triggered release system for small molecules.

At the same time, steel has been increasingly suffered from environment polluted by sulfide ions, because dissolution of metal ions from a virgin metal surface is stimulated and accelerated by formation of stable sulfides and acidic microareas induced by corrosion.[16] A similar corrosion mechanism is attributed to the inner corrosion of oil pipelines. By now, an effective method to inhibit the S^{2-}-induced corrosion was limited by forming a passive film on the substrate; whereas the protection will be no longer valid when the films are damaged (e.g., by scratching). It was found that 1*H*-benzotriazole (BTA)[17] can completely inhibit the corrosion of steel in salt water[18] as well as in acidic[19] environment. Moreover, the reversibility of the Cu-BTA complex in acidic condition was confirmed by Li and co-workers,[20] that is the insoluble structures can be redissolved in acidic condition. On the other hand, sulfide ions can easily extract the Cu^{1+} ions from the Cu-BTA complex because of the great difference between the stability constants of Cu_2S and the Cu-BTA complex (4×10^{47} and 1.54×10^{-2}, respectively).[11] Using the insoluble Cu-BTA complex at the

Z. Zheng, Dr. M. Schenderlein, Dr. D. Borisova, Prof. H. Möhwald, Dr. D. Shchukin
Max-Planck Institute of Colloids and Interfaces, 14424, Potsdam, Germany;
E-mail: zhaoliang.zheng@mpikg.mpg.de
Z. Zheng, Prof. R. Cao
State Key Laboratory of Structural Chemistry, Fujian Institute of Research on the Structure of Matter, the Chinese Academy of Sciences, 350002, Fuzhou, China
X. Huang
Fritz-Haber-Institut der MPG, Faradayweg 4-6, 14195, Berlin, Germany
Dr. D. Shchukin
Stephenson Institute for Renewable Energy
Department of Chemistry
University of Liverpool
Crown Street, Liverpool, L69 7ZD, UK

DOI: 10.1002/adfm.201203180

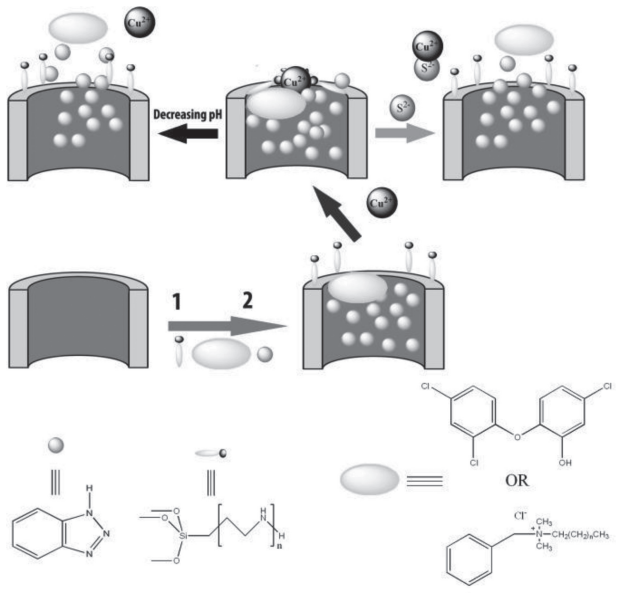

Scheme 1. Schematic representation of the procedure of forming a stimuli-triggered release system and of the stimulated release process: amino-functionalization (1) and loading forming nanovalves (2) and stimulated release.

opening of mesopores, Lvov's group[21] was able to control the release profile of BTA from halloysite nanotubes. Therefore, the insoluble Cu-BTA complex is a promising candidate to serve as pH and sulfide ion sensitive nanovalve for controlled pore opening of BTA-loaded MSNs.

In the present work, we have developed a pH/sulfide ion responsive multifunctional release system based on MSNs using an insoluble Cu-BTA complex formed at the opening of silica mesopores loaded with corrosion inhibitor (BTA) and antibacterial agent (benzalkonium chloride or triclosan, BC or TC respectively). These two active agents with different functionality can be loaded step-by-step into silica channels, trapped by the Cu-BTA complex and released in a controlled way upon local changes of pH or interaction with external sulfide ions (**Scheme 1**). To realize this, the outer surface or mesopore opening of MSNs was first functionalized with N-(3-trimethoxysilylpropyl) ethylenediamine (DiA) to form DiA-MSNs to stabilize the nanovalves formed at the opening. Then, the functionalized MSNs were loaded by BTA and biocides with different molar ratio through a vacuum method.[22] The loaded nanocontainers were recovered by centrifugation and washed (Figure S1 in the Supporting Information) to remove the excess of absorbed BTA and biocides. Finally, aqueous $CuSO_4$ solution was dropped on the powder of the loaded nanocontainers to form an insoluble complex with BTA at the opening of mesopores, obtaining Cu_x-(yTC or BC, BTA)@DiA-MSNs where x is the concentration of $CuSO_4$ solution and y is the molar ratio of biocide to BTA in the first loading cycle. The sample color changed dramatically from pale yellow to pale green, blue green or blue with the increase of the number of amino groups in one functionalizing agent (Figure S2). The release of the inhibitor and antibacterial agent was triggered when the pH was lower than 5 or $[S^{2-}]$ higher than 0.02 mM (about 0.6 ppm). All experiments of preparation, characterization, loading and release were carried out at room temperature.

2. Results and Discussion

2.1. Structural Characterization

The synthesis of the stimuli-triggered release system starts with functionalizing surface or pore opening of MSNs with one of the three aliphatic amines (aminopropyltriethoxysilane, N-(3-trimethoxysilylpropyl)ethylenediamine and N-(3-trimethoxysilylpropyl)diethylenetriamine), with the number (n) of amino groups ranging from 1 to 3, named as SingleA-, DiA- and TriA-MSNs, respectively. The amino-modification performed mainly at the openings of the mesopores was realized by temporarily leaving template material inside the porous structure during functionalization. SEM, TEM (Figure S3) images and dynamic light scattering (DLS) measurements of three types of functionalized MSNs reveal negligible differences when compared with bare ones. FTIR spectra (Figure S4), TGA analysis (Figure S5) and zeta-potential measurements (Figure S6) were employed to confirm the functionalization of MSNs with different amino-agents: TriA-MSNs have the highest density of amino groups on the surface, while DiA- and SingleA-MSNs have similar coverage but higher than the bare ones.

In addition, SingleA-MSNs have the lowest specific surface area (710 m^2/g) and pore volume (1.0 cm^3/g) in BET measurements among three functionalized and one bare sample, as shown in Table S1 and Figure S7. It is widely accepted that the surface and pore volume are of top importance to provide high loading amount of cargo molecules.[1d] Compared with DiA and TriA agents, aminopropyltriethoxysilane has a smaller molecular weight and, therefore, will easier replace the template inside the structure thus partly modifying the interior of the mesopores.[23] DiA- and TriA-MSNs have relatively large specific surface area (870 and 860 m^2/g) and almost intact pore volume (1.5 and 1.4 cm^3/g) implying the amino-functionalization mainly at the opening of the mesopores or the surface of silica.

The sequence of four samples in TGA for the actual BTA loading and release amount at equilibrium state determined by UV analysis (Table S1) is consistent with the BET results, that is bare MSNs, DiA-MSNs, TriA-MSNs and SingleA-MSNs. But for short-time release (2 h), TriA-MSNs release the smallest amount of inhibitor at pH ≈ 6–7 due to the nucleophilicity of the aliphatic amines[24] and shrinking of the pore diameter. The release profiles (Figure S8) reveal that except TriA-MSNs, the other two functionalized samples have similar release kinetics as the bare silica, which indicates an immediate release when the nanovalves are opened. Thus, among the three functionalized MSNs, DiA-MSNs possess the highest loading capacity and an ideal release profile of inhibitor for anti-corrosion self-healing.

To prevent spontaneous leakage of active species during formation of nanovalves, the insoluble Cu-BTA complex was formed and fixed at the pore opening of loaded DiA-MSNs by dropping a small volume of $CuSO_4$ aqueous solution onto powders of them. In **Figure 1**, the formation of a Cu-BTA complex

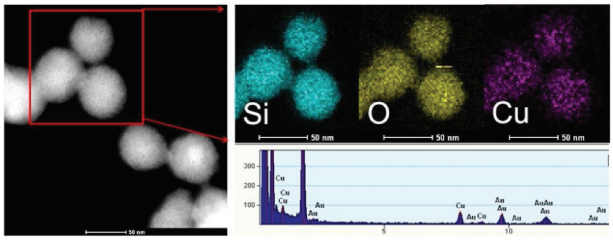

Figure 1. HAADF-STEM and elemental mapping image Cu_{60}-(0.1BC, BTA)@DiA-MSNs.

for Cu_{60}-(0.1 BC, BTA)@DiA-MSNs was confirmed by high-angle annular dark-field scanning transmission electron microscopy (HAADF-STEM) imaging and elemental mapping, in which Cu is exclusively located on the loaded DiA-MSNs, indicating the stabilization of nanovalves at the pore opening of MSNs and prevention of spontaneous leakage of BTA. For comparison, the location of the insoluble complex after dropping of $CuSO_4$ aqueous solution onto (0.1BC, BTA)@MSNs was also examined. As revealed in Figure S9, copper cannot be fixed only on MSNs, but also forms a considerable number of free NPs with BTA. The above observation stresses the important role of DiA functionalization in stabilizing nanovalves at the surface of MSNs. On the other hand, we tried to form nanovalves with conventional methods, for example, dispersing 16 mg of loaded DiA-MSNs in 20 mL of $CuSO_4$ aqueous solution with different concentrations. The spontaneous leakage of inhibitors was determined by analyzing the supernatant with UV at 275 nm. The leakage composition is 0.47, 0.29, 0.25, 0.18, and 0.05 of the actual loading for 20, 40, 60, 80, and 160 mM (concentration of $CuSO_4$) even not including BTA forming an insoluble complex outside the mesopores.

2.2. Responsive Release Performance

As shown in **Figure 2**, the premature release of Cu_x-(BTA)@DiA-MSNs was examined at first. The complex itself without any additive cannot completely prevent the premature release. The release amount is decreased when the concentration of $CuSO_4$ solution increases from 20 to 80 mM but rises as 160 mM is employed. As we just dropped $CuSO_4$ solution onto pure BTA crystals with the same weight as one loaded in DiA-MSNs, no free BTA was detected in UV even at lowest $CuSO_4$ concentration (20 mM) used, which implies the formation of a supramolecular network composed of cupric ions and BTA.[25] To clarify the role of the Cu-BTA supramolecules in our system on formation of nanovalves at the openings of the mesopores, the cupric loading was measured by detecting the metal content in Cu_x-(BTA)@DiA-MSNs. ICP reveals that, except for the highest concentration (160 mM) which yields 1.5 wt% cupric loading in Cu_{160}-(BTA)@DiA-MSNs, only about 0.8 wt% can be obtained from the other 4 diluted $CuSO_4$ solutions. The hydrophobicity of Cu-BTA complex network formed at the openings prohibits further flow-in of cupric ions. However, the concentration of 160 mM may not result in a network, which, to some extent, allows free flow-in of cupric ions through the openings. Furthermore, a lot of uniform NPs can be observed outside the MSNs in

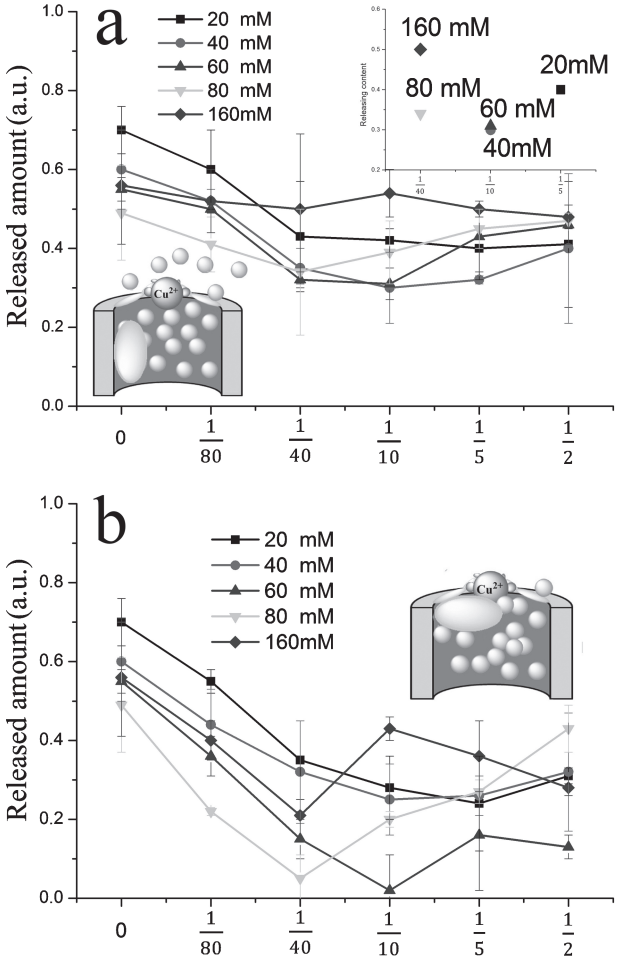

Figure 2. Premature release of BTA from a) Cu_x-(γTC, BTA)@DiA-MSNs and b) Cu_x-(γBC, BTA)@DiA-MSNs depending on the ratio of TC or BC to BTA (*x* axis) and concentration of copper sulfate solution for formation of nanovalves. The inset in (a) indicates the lowest premature release level of five Cu_x-(γTC, BTA)@DiA-MSNs samples (x = 20, 40, 60, 80, and 160) with different TC/BTA ratios.

the TEM image of Cu_{160}-(BTA)@DiA-MSNs (Figure S10). Our results agree very well with the conclusion of Li and coworkers, in which linkages among NPs provided by BTA are found to be formed when the sample contains low cupric and high BTA concentrations, but the particles appear to be to more discrete if low concentration of BTA reacts with a high concentration of cupric ions.[25]

In the next step of the formation of multifunctional nanocontainers, we introduced two kinds of biocide agents (benzalkonium chloride or triclosan, BC or TC respectively) into the nanocontainers, which not only extended the application of MSNs to antibacterial activity but also prevented premature release of inhibitors. TC has low solubility in water but is soluble in organic solvents, e.g., acetone. BC, on the contrary, is a wide-range antibacterial agent and easily soluble in water. Thus, insoluble TC in mesopores can serve as fixed barrier for flow-out of BTA in water, while BC can freely move in the confined

space and easily block the space between the complex networks or between network and wall of pores. Figure 2a shows that TC can further decrease the premature release of BTA to the lowest level of around 30% for Cu_{40}-(0.1TC, BTA) and Cu_{60}-(0.1TC,BTA)@DiA-MSNs. The lowest premature release for all Cu_x-(γTC, BTA)@DiA-MSNs is also closely related to the concentration of $CuSO_4$ solution (Figure 2a, inset). For a higher concentration (e.g., 80 or 160 mM), the lowest premature release is achieved for the sample with a higher content of BTA (e.g., 0.025TC) and vice versa. On the contrary, the uncontrolled release of BTA can be well prevented when water soluble BC is applied. In Figure 2b a similar release profile as for TC samples can be seen but with a more dramatic decrease in release of BTA. The premature release can be minimized to the lowest level of 0.02 for Cu_{60}-(0.1BC, BTA)@DiA-MSNs. As the insoluble complex Cu-BTA has been formed at the openings of the mesopores, the pore diameter shrinks to <1 nm as determined by BET measurement. BC has larger molecular weight and volume than BTA, which clogs the opening of such a small pore. As a result, the release of BTA is sharply decreased or even prevented. This explanation is derived purely from geometric kinetic constraints[26] without consideration of the interaction between carrier and cargo. However, it is reasonable in our system because BTA and silica have the same charge in a wide pH range and BC is freely moving in the confined space.

We conducted stimuli-triggered release experiments using Cu_{60}-(0.1BC, BTA)@DiA-MSNs. The release of BTA from the samples was monitored by measuring the fluorescence intensity of the released inhibitor as a function of time (Figure S11). Comparing with the release profile without nanovalves, a flat baseline (**Figure 3**a) shows that BTA molecules are entrapped within the functionalized MSNs under neutral aqueous conditions (pH ≈ 6.5–8) without any premature release. The pH value of the solution was then lowered down below 5 to stimulate the release of BTA. As compared with the released amount from DiA-MSNs without nanovalves in 24 h (equilibrium released amount), 85% and 80% release of the loaded BTA were achieved in 100 min when the pH value was 3 and 4, respectively. Even the higher value (pH = 5) can also induce 50% release of BTA.

To confirm S^{2-}-responsive release of inhibitor, the samples were immersed in Na_2S solutions with four different concentrations, during which the fluorescence intensity of the released inhibitor as a function of time has been tracked. Figure 3b shows that spontaneous release happened once the sample was immersed in Na_2S solution with a higher concentration (2 and 1 mM). More than half of the release can be observed even if the solvent is diluted by 100 times (to 0.02 mM).

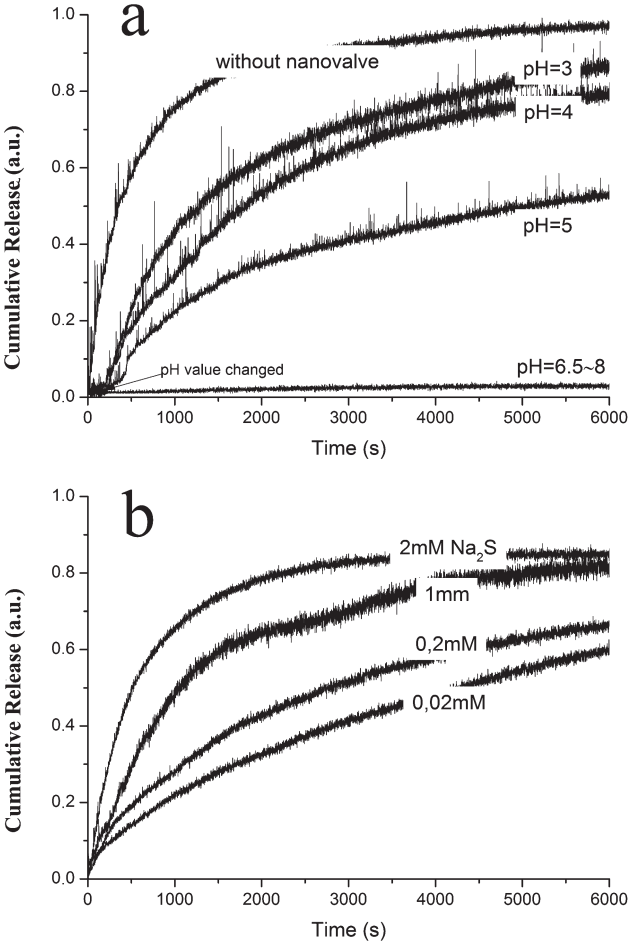

Figure 3. Release profiles of BTA from Cu_{60}-(0.1BC, BTA)@DiA-MSNs at a) different pH values and b) different concentration of sulfide ions.

2.3. Anticorrosion and Antifouling Performance

To confirm the specific corrosion protection provided by the stimulated release system, current density measurements were carried out in 0.1 M NaCl aqueous solution employing the scanning vibrating electrode technique (SVET). Steel substrates were coated with a polyester layer incorporating BTA, (0.1BC, BTA)@DiA-MSNs and Cu_{60}-(0.1BC, BTA)@DiA-MSNs nanocontainers, respectively. SVET measurements were conducted to detect the current density around the scratched region.[27] Prior to measurement, scratches were deliberately made with a scalpel without spoiling the metal surface. As shown in Figure S12, the coating impregnated with (0.1BC, BTA)@DiA-MSNs and Cu_{60}-(0.1BC, BTA)@DiA-MSNs can effectively inhibit the corrosion as compared with the one purely doped with BTA. When the neutral 0.1 M NaCl solution was tuned to pH = 5, a dramatic difference between two samples with or without Cu-BTA complex as nanovalves is revealed in **Figure 4**. The sample with specifically responsive nanovalves exhibits an obvious feedback protection offered by stimulated release of BTA. At the time of 70 min corrosion is detected in both samples with similar current density around 2.5 μA/cm^2. However, after 4 h, the corrosion signal of the Cu_{60}-(0.1BC, BTA)@DiA-MSNs sample decreased below 1 μA/cm^2. On the contrary, the current density of the (0.1BC, BTA)-DiA-MSNs sample (without nanovalves) increases to 4 μA/cm^2. In addition, the time-resolved change of anodic and cathodic current within the measured region also reveals the great contrast between the above two samples. In another much more corrosive condition at the salt solution containing sulfide ions with [S^{2-}] = 0.02 mM, Cu_{60}-(0.1BC, BTA)@DiA-MSNs exhibit an outstanding corrosion-resistant efficiency. In **Figure 5**a, a very broad and high anodic peak (13 μA/cm^2)

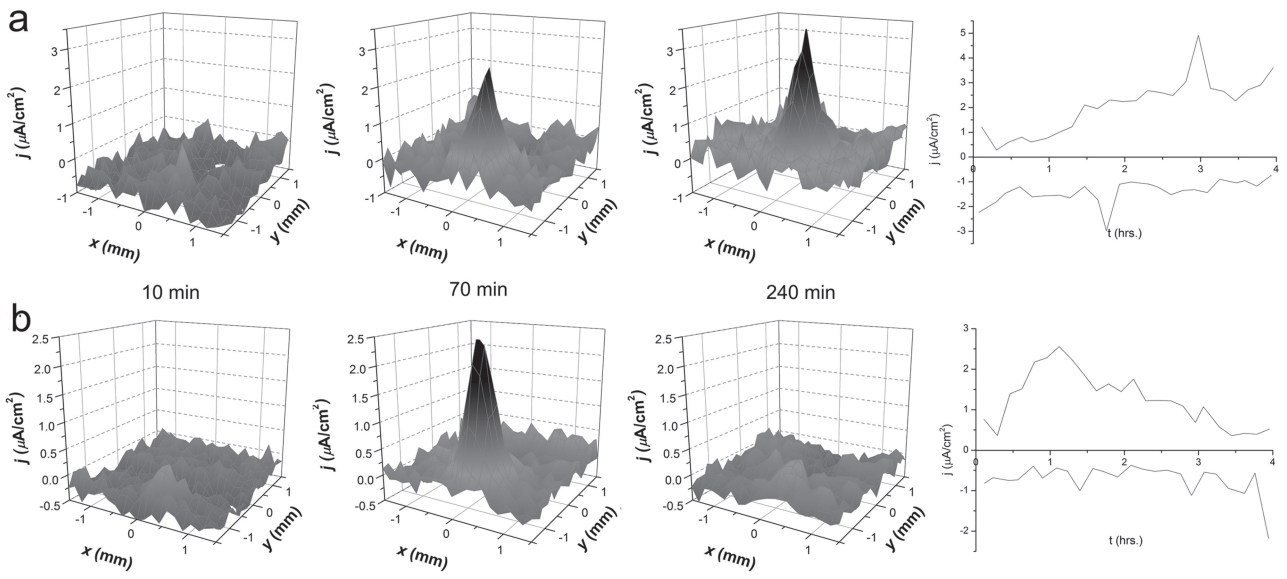

Figure 4. SVET current density maps of steel coated with polyester coating containing a) (0.1BC, BTA)@DiA-MSNs and b) Cu_{60}-(0.1BC, BTA)@DiA-MSNs in 0.1 M NaCl (pH = 5). Right: maximum and minimum current densities (*j*) versus time after submersion in 0.1 M NaCl (pH = 5) over the scratched surface of the polyester coating with corresponding current density maps on the left.

can be seen in the current density map for the sample without responsive nanovalves during submersion for 4 h. In the case of the sample with nanovalves, there is a small positive peak (Figure 5b), indicating that almost no metallic ions are produced by oxidation on the corrosion anode. From the optical observation of the scratched area after corrosion tests (Figure 5, right), one can deduce that with stimuli-triggered release of BTA the Cu_{60}-(0.1BC, BTA)@DiA-MSNs sample can effectively prevent the synergistic corrosion induced by sulfide ions and sodium chloride.

To further assess the specific protection efficiency of the feedback coatings, samples with BTA, (0.1BC, BTA)@DiA-MSNs and Cu_{60}-(0.1BC, BTA)@DiA-MSNs were first immersed in 0.1 M NaCl solution for 1 day, then in 0.1M NaCl solution with pH = 5 or $[S^{2-}]$ = 0.02 mM for another day. A defect on the coating was made as explained before. After the 1st day, the destructive corrosion effect can already be clearly observed on the substrates protected by the coating directly doped with BTA. After the second cycle in more corrosive condition, (0.1BC, BTA)@DiA-MSNs sample showed some expansion in the scratch as well as notable corrosion products (**Figure 6**) while the scratch on the Cu_{60}-(0.1BC, BTA)@DiA-MSNs sample seems to be intact. This obvious difference between the sample with nanovalves and the one without or just doped with BTA confirms the highly specific and long-term anticorrosion efficiency of such hybrid coatings incorporating nanocontainers which have the ability of stimuli-triggered release of small molecular inhibitors.

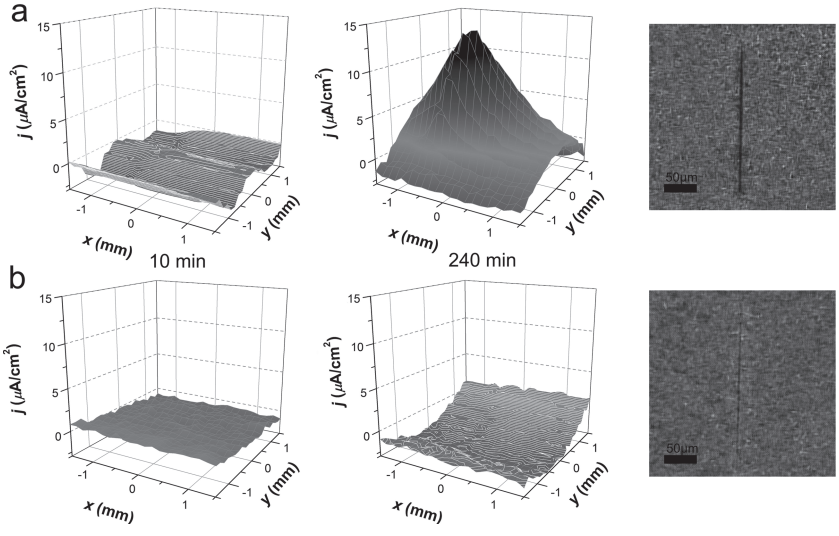

Figure 5. SVET current density maps of steel coated with polyester coating containing a) (0.1BC, BTA)@DiA-MSNs and b) Cu_{60}-(0.1BC, BTA)@DiA-MSNs in 0.1 M NaCl and $[S^{2-}]$ = 0.02 mM). Right: optical observation of scratches after 240 min of submersion.

Additionally, electrochemical impedance spectroscopy (EIS) was employed to evaluate the barrier properties of the coating. The corrosion tests for the intact coatings on steel substrates were carried out in 1 M NaCl aqueous solution. The results after one and 21 days of submersion are presented in **Figure 7**a. The (0.1BC, BTA)@DiA-MSNs sample exhibits a notable sign of corrosion after three-week submersion as it is seen from the drop ($10^{7.5}$ to 10^4) of the absolute impedance (|Z|) in Bode plots. On the other hand, the Cu_{60}-(0.1BC, BTA)@DiA-MSNs sample exhibits an acceptable coating barrier property due to its small decrease in absolute impedance value (by only one order of magnitude) in Figure 7b. Photographs of the coated metal substrates after three-weeks

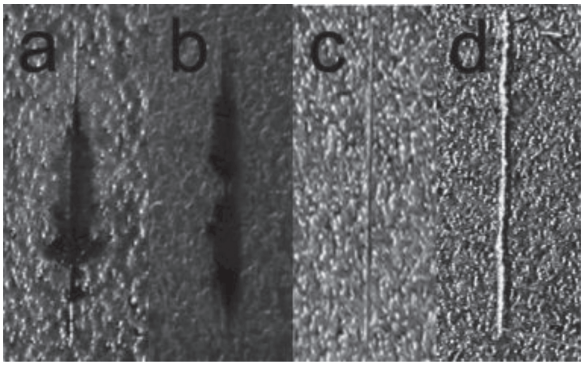

Figure 6. Optical observation of a steel substrate coated with polyester coating impregnated with a,b) (0.1BC, BTA)@DiA-MSNs and c,d) Cu_{60}-(0.1BC, BTA)@DiA-MSNs (nanocontainers with sensitive nanovalves) after successive 1 day of submersion in 0.1 M NaCl and 1 day in 0.1 M NaCl with (a, c) pH = 5 and (b, d) $[S^{2-}] = 0.02$ mM.

submersion in the salt solution also show the difference in barrier properties (Figure 7a,b). In agreement with the EIS measurements, the (0.1BC, BTA)@DiA-MSNs sample was severely corroded with a large amount of corrosion product and bubbles in the coating. The sample with specifically responsive nanovalves (Cu-BTA complex) almost keeps the integrity of the coating with the appearance of a small amount of corrosion product, which can be attributed to non-ideal dispersibility of modified MSNs in hybrid coatings. As the premature release of BTA cannot be prevented completely when (0.1BC, BTA)@DiA-MSNs were incorporated in the coating matrix, the effective coverage of substrate using polyester coating is hindered by the strong chemical bonding of the inhibitor with iron under the coating, which induces insufficient passivation during the corrosion process.[28]

The second, antifouling, functionality of the coating was demonstrated by the release of the biocide, benzalkonium chloride, from Cu_{60}-(0.1BC, BTA)@DiA-MSNs confirming the multifunctionality of the coating with anticorrosion and antifouling/antibacteria effect. **Figure 8** shows the images of E.Coli colonies after treatment with scratched coated steel substrates containing Cu_{60}-(BTA)@DiA-MSNs and Cu_{60}-(0.1BC, BTA)@DiA-MSNs for 20 h. It is obvious that the activity of E.Coli is suppressed by BC which was released from the nanocontainers resulting in much less colonies when compared with coating without antibacterial agent. Furthermore, the antifouling effect of the multifunctional coating is also visible in Figure 8c where a dense biofilm adhered onto the coatings without BC-loaded nanocontainers. On the contrary, there is only a very thin biofilm seen on the multifunctional coating containing Cu_{60}-(0.1BC, BTA)@DiA-MSNs.

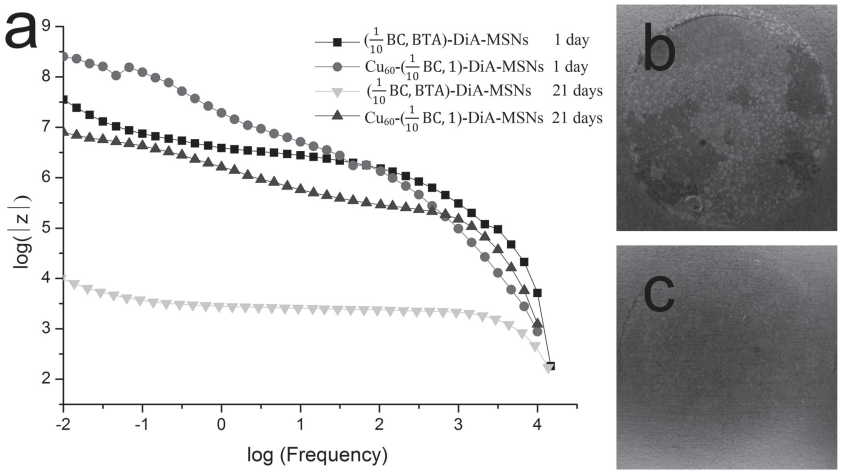

Figure 7. a) Bode plot showing the influence of the frequency of the applied potential on the absolute impedance, |z|, of the coated steel substrates after 1 and 21 days in aqueous 1 M NaCl. Optical observation of a steel substrate coated with polyester coating impregnated with b) (0.1BC, BTA)@DiA-MSNs and c) Cu_{60}-(0.1BC, BTA)@DiA-MSNs after 21 days of submersion.

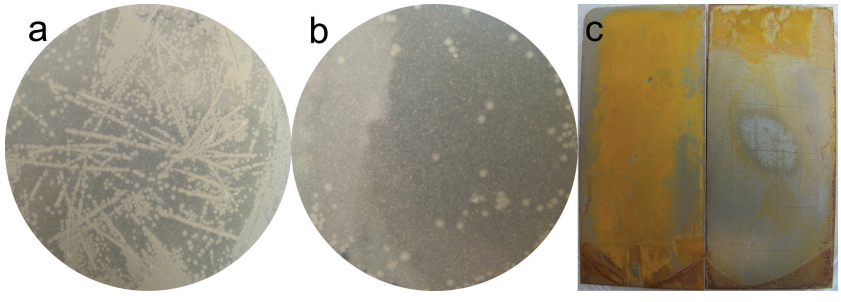

Figure 8. Images of E.Coli colonies after treatment with scratched coated steel substrates containing a) Cu_{60}-(BTA)@DiA-MSNs and b) Cu_{60}-(0.1BC, BTA)@DiA-MSNs for 20 h and c) images of steel coated with polyester coating containing Cu_{60}-(BTA)@DiA-MSNs and Cu_{60}-(0.1BC, BTA)@DiA-MSNs after 20 h. The yellow coating on the steel plate is E.Coli's biofilm. The left plate with thick biofilm was not protected by antifouling agent released from the nanocontainers; whereas the one on the right with antifouling protection was coated only with a thin film.

3. Conclusions

In conclusion, a pH/sulfide ion responsive release system was demonstrated, which is based on mesoporous silica nanoparticles using an insoluble Cu-BTA complex as a nanovalve formed at the openings of mesopores into which benzotriazole (corrosion inhibitor) and benzalkonium chloride (biocide) were loaded. The spontaneous leakage and premature release of active species was completely avoided during the procedure of coating formation. The responsive release system opens when the pH is lower than 5 or $[S^{2-}]$ is higher than 0.02 mM (about 0.6 ppm). Containing the responsive release system, the hybrid coating exhibits anticorrosion self-healing property in response to pH lowering and presence of sulfide ions also maintaining a high level barrier level. Due to incorporation of biocide in the release

system, the coating is also provided with a second, antifouling effect. This work opens a way for a multifunctional controlled release system, which can be obtained just by adding another active agent in the loading procedure for nanocontainers.

4. Experimental Section

Synthesis Method: Silica mesoporous nanoparticles (MSNs) with cetyltrimethylammonium chloride (CTACl) template were fabricated according to the method described in ref. [2a]. After vacuum drying, 100 mg of MSNs with CTACl were mixed with 20 mL of anhydro-ethanol under the protection of nitrogen. The mixture was vigorously stirred for 30 min and then about 7 µL of amino-agent (aminopropyltriethoxysilane, N-(3-trimethoxysilylpropyl)ethylenediamine and N-(3-trimethoxysilylpropyl)diethylenetriamine), SingleA, DiA or TriA with the same molar concentration) was injected. The mixture was left stirring for another 20 h to fully functionalize the surface of MSNs. The white powder was collected with centrifugation and washed with ethanol. The following template extraction was conducted in ethanol/HCl mixture (15 mL HCl (37%)/150 mL ethanol) under ultrasonic agitation (100 W, 35 kHz).

Loading and Preparation of Nanovalves: The loading of the silica containers with BTA/BC was conducted under reduced pressure (30 mbar). For the first loading cycle, 40 mg of as-synthesized nanocontainers were dispersed in the solution with saturated amount of aqueous BTA solution and desired concentration of BC. The mixture was stirred in vacuum for 2 hrs. For another two loading cycles, only saturated aqueous BTA solution was applied to locate BTA at the openings of the mesopores. For BTA/TC loading, the solvent was replaced by acetone. To obtain "clean" loaded nanocontainers without absorbed BTA and BC, a quick washing method was developed to prevent spontaneous leakage of the loaded active compounds to the maximum extent. As shown in Figure S1, the home-made washing machine was simply composed of a piece of filter paper with a transparency of 0.05 µm, a funnel and a pump. Before washing, a thin layer of pristine solid was carefully deposited on the filter paper. Then water was added on the solid droplet. The procedure was cycled for several times till the released amount of BTA (determined by UV analysis) remained constant.

Then, 0.8 mL of copper sulfate aqueous solution with different concentrations (20, 40, 60, 80, and 160 mM) was dropped on the "clean" nanocontainers (160 mg). The resulting powder was dried in a desiccator overnight.

Coating Formation: The dispersion of loaded nanocontainers in primer solvent (10 wt%) was added directly to the polyester mixed primer solution to facilitate their dispersion. To prepare a coating with Cu_{60}-(0.1BC, BTA)@DiA-MSNs, 200 mg of powder was added to the primer polyester solution (20 g). To prepare a BTA-doped coating, a 1 wt% solution of BTA in solvent (2 g) was added to the polyester primer (20 g). In all cases the samples were shaken thoroughly in order to homogeneously disperse the nanocontainers or BTA. Samples were coated on the steel substrates (scrubbed clean with EtOH, then ethyl acetate) using a Bungard RDC 15 dip coater (immersion time 3 min) and cured at 200 °C (6 min).

Characterization: IR spectroscopy (Bruker IFS 66 FT-IR spectrometer), BET (Macromeritics TriStar 3000 system), DLS (Malvern Zetasizer 4), SEM (Hitachi S-4800), optical microscopy and TEM (Zeiss EM912) were used to characterize the structure of the samples. HADDF STEM image and STEM EDX mapping were recorded from Cs–corrected Titan 80–300 microscopes operated at 300 kV. An Agilent 7500 CS ICP mass spectrometer was employed to determine the copper content in solid sample.

UV-vis spectroscopy (8453 UV-visible spectrophotometer, Agilent technologies) and fluorescence spectroscopy were applied to determine the release profile of BTA using the spectroscopic setup shown in Figure S11. The 1.6 mg powder was placed in the bottom of a small bag which is made of a dialysis membrane. Then, distilled H_2O (at pH ≈ 7; 4 mL) was added to the cuvette till the bottom of the bag was immersed into water. A 5-mm stirring bar was added to the cuvette. The solution in the cuvette was stirred vigorously to quickly balance the concentration of the releasing BTA. The solution was monitored using a CCD detector, which collected the emission spectra of the solution. A laser probe beam directed into the solution at 2 cm above the bottom and around 1 cm below the top of the cuvette was used to excite the released BTA molecules. The fluorescence spectra of the released anticorrosion agent were collected at 1 s intervals during the whole duration of the experiment. The fluorescence intensity at the emission maximum of BTA was plotted as a function of time in order to generate a release profile. The concentration of BTA was finally determined by UV spectroscopy. Stimulated release of BTA from the silica was accomplished by adding neutral solution into the one with lower pH value or into a solution with different concentration of Na_2S.

For the characterization and quantification of the corrosion process in dip-coated steel substrates, the scanning vibrating electrode technique (SVET, Applicable Electronics) and short-time impedance spectroscopy (EIS, Ivium technologies) were employed. Detailed information can be seen in previous papers of our group.[2]

Supporting Information

Supporting Information is available from the Wiley Online Libray or from the author.

Acknowledgements

We thank Dr. Wenbin Zhou in Max Planck Institute of Molecular Plant Physiology for the antifouling experiment. This work was financially supported by joint Ph.D. programme of Chinese Acadamy of Sciences and Max-Planck Society, EU FP7 Nanomar project and 973 Program (2011CB932504).

Received: October 30, 2012
Published online: February 13, 2013

[1] a) S. Saha, K. C. F. Leung, T. D. Nguyen, J. F. Stoddart, J. I. Zink, *Adv. Funct. Mater.* **2007**, *17*, 685–693; b) M. W. Ambrogio, C. R. Thomas, Y. L. Zhao, J. I. Zink, J. F. Stoddartt, *Acc. Chem. Res.* **2011**, *44*, 903–913; c) Z. X. Li, J. C. Barnes, A. Bosoy, J. F. Stoddart, J. I. Zink, *Chem. Soc. Rev.* **2012**, *41*, 2590–2605; d) M. Vallet-Regi, F. Balas, D. Arcos, *Angew. Chem. Int. Ed.* **2007**, *46*, 7548–7558; e) M. Vallet-Regi, I. Izquierdo-Barba, M. Colilla, *Philos. Trans. R. Soc., A* **2012**, *370*, 1400–1421.

[2] a) D. Borisova, H. Mohwald, D. G. Shchukin, *ACS Nano* **2011**, *5*, 1939–1946; b) M. J. Hollamby, D. Fix, I. Donch, D. Borisova, H. Mohwald, D. Shchukin, *Adv. Mater.* **2011**, *23*, 1361–1365.

[3] a) J. Lee, J. Kim, T. Hyeon, *Adv. Mater.* **2006**, *18*, 2073–2094; b) A. Stein, *Adv. Mater.* **2003**, *15*, 763–775.

[4] a) A. Schlossbauer, S. Warncke, P. M. E. Gramlich, J. Kecht, A. Manetto, T. Carell, T. Bein, *Angew. Chem.* **2010**, *122*, 4842–4845; b) A. Schlossbauer, S. Warncke, P. M. E. Gramlich, J. Kecht, A. Manetto, T. Carell, T. Bein, *Angew. Chem. Int. Ed.* **2010**, *49*, 4734–4737; c) E. Aznar, L. Mondragón, J. V. Ros-Lis, F. Sancenón, M. D. Marcos, R. Martínez-Máñez, J. Soto, E. Pérez-Payá, P. Amorós, *Angew. Chem.* **2011**, *123*, 11368–11371; d) E. Aznar, L. Mondragón, J. V. Ros-Lis, F. Sancenón, M. D. Marcos, R. Martínez-Máñez,

J. Soto, E. Pérez-Payá, P. Amorós, *Angew. Chem. Int. Ed.* **2011**, *50*, 11172–11175.

[5] a) C. Park, K. Oh, S. C. Lee, C. Kim, *Angew. Chem.* **2007**, *119*, 1477–1479; b) S. Angelos, Y.-W. Yang, K. Patel, J. F. Stoddart, J. I. Zink, *Angew. Chem.* **2008**, *120*, 2254–2258; c) S. Angelos, Y.-W. Yang, K. Patel, J. F. Stoddart, J. I. Zink, *Angew. Chem. Int. Ed.* **2008**, *47*, 2222–2226; d) L. Du, S. Liao, H. A. Khatib, J. F. Stoddart, J. I. Zink, *J. Am. Chem. Soc.* **2009**, *131*, 15136–15142; e) H. P. Rim, K. H. Min, H. J. Lee, S. Y. Jeong, S. C. Lee, *Angew. Chem. Int. Ed.* **2011**, *50*, 8853–8857.

[6] a) C.-Y. Lai, B. G. Trewyn, D. M. Jeftinija, K. Jeftinija, S. Xu, S. Jeftinija, V. S. Y. Lin, *J. Am. Chem. Soc.* **2003**, *125*, 4451–4459; b) T. D. Nguyen, H.-R. Tseng, P. C. Celestre, A. H. Flood, Y. Liu, J. F. Stoddart, J. I. Zink, *Proc. Natl. Acad. Sci. USA* **2005**, *102*, 10029–10034; c) K. Patel, S. Angelos, W. R. Dichtel, A. Coskun, Y.-W. Yang, J. I. Zink, J. F. Stoddart, *J. Am. Chem. Soc.* **2008**, *130*, 2382–2383; d) M. W. Ambrogio, T. A. Pecorelli, K. Patel, N. M. Khashab, A. Trabolsi, H. A. Khatib, Y. Y. Botros, J. I. Zink, J. F. Stoddart, *Org. Lett.* **2010**, *12*, 3304–3307.

[7] a) Y. Zhu, M. Fujiwara, *Angew. Chem.* **2007**, *119*, 2291–2294; b) Y. Zhu, M. Fujiwara, *Angew. Chem. Int. Ed.* **2007**, *46*, 2241–2244; c) S. Angelos, E. Choi, F. Vögtle, L. De Cola, J. I. Zink, *J. Phys. Chem. C* **2007**, *111*, 6589–6592; d) D. P. Ferris, Y.-L. Zhao, N. M. Khashab, H. A. Khatib, J. F. Stoddart, J. I. Zink, *J. Am. Chem. Soc.* **2009**, *131*, 1686–1688; e) J. L. Vivero-Escoto, I. I. Slowing, C.-W. Wu, V. S. Y. Lin, *J. Am. Chem. Soc.* **2009**, *131*, 3462–3463.

[8] a) K. C. F. Leung, T. D. Nguyen, J. F. Stoddart, J. I. Zink, *Chem. Mat.* **2006**, *18*, 5919–5928; b) C.-L. Zhu, C.-H. Lu, X.-Y. Song, H.-H. Yang, X.-R. Wang, *J. Am. Chem. Soc.* **2011**, *133*, 1278–1281.

[9] C. Wang, Z. Li, D. Cao, Y.-L. Zhao, J. W. Gaines, O. A. Bozdemir, M. W. Ambrogio, M. Frasconi, Y. Y. Botros, J. I. Zink, J. F. Stoddart, *Angew. Chem. Int. Ed.* **2012**, *51*, 5460–5465.

[10] a) T. D. Nguyen, K. C. F. Leung, M. Liong, C. D. Pentecost, J. F. Stoddart, J. I. Zink, *Org. Lett.* **2006**, *8*, 3363–3366; b) T. D. Nguyen, Y. Liu, S. Saha, K. C. F. Leung, J. F. Stoddart, J. I. Zink, *J. Am. Chem. Soc.* **2007**, *129*, 626–634.

[11] N. K. Allam, A. A. Nazeer, E. A. Ashour, *J. Appl. Electrochem.* **2009**, *39*, 961–969.

[12] K. K. Coti, M. E. Belowich, M. Liong, M. W. Ambrogio, Y. A. Lau, H. A. Khatib, J. I. Zink, N. M. Khashab, J. F. Stoddart, *Nanoscale* **2009**, *1*, 16–39.

[13] F. Muhammad, M. Guo, W. Qi, F. Sun, A. Wang, Y. Guo, G. Zhu, *J. Am. Chem. Soc.* **2011**, *133*, 8778–8781.

[14] J. L. Vivero-Escoto, I. I. Slowing, C. W. Wu, V. S. Y. Lin, *J. Am. Chem. Soc.* **2009**, *131*, 3462.

[15] C. Y. Lai, B. G. Trewyn, D. M. Jeftinija, K. Jeftinija, S. Xu, S. Jeftinija, V. S. Y. Lin, *J. Am. Chem. Soc.* **2003**, *125*, 4451–4459.

[16] G. S. Eklund, *J. Electrochem. Soc.* **1974**, *121*, 467–473.

[17] F. M. Al-Kharafi, A. M. Abdullah, B. G. Ateya, *Electrochem. Solid-State Lett.* **2006**, *9*, B19-B23.

[18] a) N. K. Allam, E. A. Ashour, H. S. Hegazy, B. E. El-Anadouli, B. G. Ateya, *Corros Sci* **2005**, *47*, 2280–2292; b) N. K. Allam, H. S. Hegazy, E. A. Ashour, *Int. J. Electrochem. Sci.* **2007**, *2*, 549–562; c) J. M. Maciel, R. F. V. V. Jaimes, P. Corio, J. C. Rubim, P. L. Volpe, A. Agostinho, S. M. L. Agostinho, *Corros. Sci.* **2008**, *50*, 879–886.

[19] S. H. Sanad, H. Abbas, A. A. Ismail, K. M. Elsobki, *Surf. Technol.* **1985**, *25*, 39–48.

[20] a) Y. Li, M. L. Gong, K. Ramji, Y. Z. Li, *J. Phys. Chem. C* **2009**, *113*, 18003–18013; b) C. Sease, *Stud. Conserv.* **1978**, *23*, 76–85.

[21] a) E. Abdullayev, R. Price, D. Shchukin, Y. Lvov, *ACS Appl. Mater. Interfaces* **2009**, *1*, 1437–1443; b) E. Abdullayev, Y. Lvov, *J. Nanosci. Nanotechnol.* **2011**, *11*, 10007–10026; c) E. Abdullayev, Y. Lvov, *J. Mater. Chem.* **2010**, *20*, 6681–6687.

[22] a) J. Lu, M. Liong, J. I. Zink, F. Tamanoi, *Small* **2007**, *3*, 1341–1346; b) M. Vallet-Regí, F. Balas, D. Arcos, *Angew. Chem.* **2007**, *119*, 7692–7703; c) Y. Hu, K. Cai, Z. Luo, K. D. Jandt, *Adv. Mater.* **2010**, *22*, 4146–4150.

[23] J. Kecht, A. Schlossbauer, T. Bein, *Chem. Mat.* **2008**, *20*, 7207–7214.

[24] M. Comes, M. D. Marcos, R. Martinez-Manez, F. Sancenon, L. A. Villaescusa, A. Graefe, G. J. Mohr, *J. Mater. Chem.* **2008**, *18*, 5815–5823.

[25] Y. Li, M. Gong, K. Ramji, Y. Li, *J. Phys. Chem. C* **2009**, *113*, 18003–18013.

[26] R. S. Shaw, N. Packard, M. Schroter, H. L. Swinney, *Proc. Natl. Acad. Sci. USA* **2007**, *104*, 9580–9584.

[27] a) H. S. Isaacs, *J. Electrochem. Soc.* **1991**, *138*, 722–728; b) R. Akid, M. Garma, *Electrochim. Acta* **2004**, *49*, 2871–2879.

[28] D. Raps, T. Hack, J. Wehr, M. L. Zheludkevich, A. C. Bastos, M. G. S. Ferreira, O. Nuyken, *Corros. Sci.* **2009**, *51*, 1012–1021.